

# Identification of CDK4/6 Inhibitors as Small Molecule NLRP3 Inflammasome Activators that Facilitate IL-1 $\beta$ Secretion and T Cell Adjuvanticity

Published as part of *Journal of Medicinal Chemistry* special issue "Medicinal Chemistry of Next Generation Vaccine Adjuvants".

Adam M. Weiss, Marcos A. Lopez II, Matthew G. Rosenberger, Jeremiah Y. Kim, Jingjing Shen, Qing Chen, Trevor Ung, Udoka M. Ibeh, Hannah Riley Knight, Nakisha S. Rutledge, Bradley Studnitzer, Stuart J. Rowan, and Aaron P. Esser-Kahn\*



Cite This: *J. Med. Chem.* 2024, 67, 14974–14985



Read Online

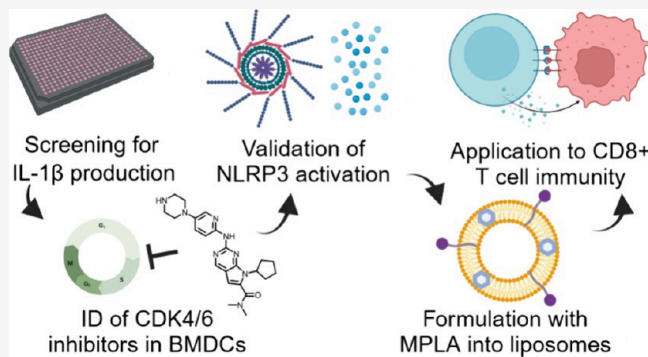
ACCESS |

Metrics & More

Article Recommendations

Supporting Information

**ABSTRACT:** Several FDA-approved adjuvants signal through the NLRP3 inflammasome and IL-1 $\beta$  release. Identifying small molecules that induce IL-1 $\beta$  release could allow targeted delivery and structure–function optimization, thereby improving safety and efficacy of next-generation adjuvants. In this work, we leverage our existing high throughput data set to identify small molecules that induce IL-1 $\beta$  release. We find that ribociclib induces IL-1 $\beta$  release when coadministered with a TLR4 agonist in an NLRP3- and caspase-dependent fashion. Ribociclib was formulated with a TLR4 agonist into liposomes, which were used as an adjuvant in an ovalbumin prophylactic vaccine model. The liposomes induced antigen-specific immunity in an IL-1 receptor-dependent fashion. Furthermore, the liposomes were coadministered with a tumor antigen and used in a therapeutic cancer vaccine, where they facilitated rejection of E.G7-OVA tumors. While further chemical optimization of the ribociclib scaffold is needed, this study provides proof-of-concept for its use as an IL-1 producing adjuvant in various immunotherapeutic contexts.



Downloaded via UNIV OF CHICAGO on January 10, 2025 at 21:30:22 (UTC).  
See https://pubs.acs.org/sharingguidelines for options on how to legitimately share published articles.

## INTRODUCTION

Despite progress in developing novel platforms for vaccination, new adjuvants that can safely and robustly stimulate adaptive immune responses are still needed.<sup>1</sup> Some of the most potent FDA-approved adjuvants, saponins, mediate their adjuvanticity in part via activation of inflammasomes and subsequent secretion of IL-1 cytokines (IL-1 $\alpha$ , IL-1 $\beta$ , IL-18, and others).<sup>1–4</sup>

Inflammasomes are innate immune danger sensors that, when activated, form polyprotein complexes that catalyze the activation of caspase 1 (Casp1).<sup>5</sup> Casp1, in the presence of a priming signal such as a Toll-like receptor 4 (TLR4) agonist, cleaves pro-IL-1 cytokines to their active form to induce potent inflammatory signaling. Casp1 also induces a regulated form of inflammatory cell death, termed pyroptosis, through gasdermin D (GSDMD) N-terminal cleavage.<sup>5</sup> Chronic IL-1 secretion is associated with various disease pathologies,<sup>6–9</sup> but acute production promotes a T<sub>H</sub>1-biased immune response to afford pathogen clearance in the context of both infection and prophylaxis.<sup>5,10</sup> Saponin-containing adjuvant formulations, such as AS01<sub>B</sub>, ALF-Q, and Matrix-M, are used in an increasing

number of vaccines despite reactogenicity in many individuals.<sup>11–14</sup> Furthermore, saponins are chemically complex and require extraction from the bark of *Quillaja saponaria*, a limited natural resource, limiting scalable production.<sup>15,16</sup> As such, it is desirable to identify new IL-1 producing adjuvants with greater safety, scalable synthesis, and chemical tunability for use in vaccination.

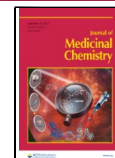
Many novel adjuvants have been identified via high throughput screening.<sup>17–19</sup> The Esser-Kahn group recently generated a high throughput data set wherein two functional outputs, transcription factor activation and cytokine production, were assayed *in vitro* following coadministration of >10,000 drug-like small molecules with PRR agonists.<sup>20</sup> One surprising

Received: February 29, 2024

Revised: July 10, 2024

Accepted: August 8, 2024

Published: August 20, 2024



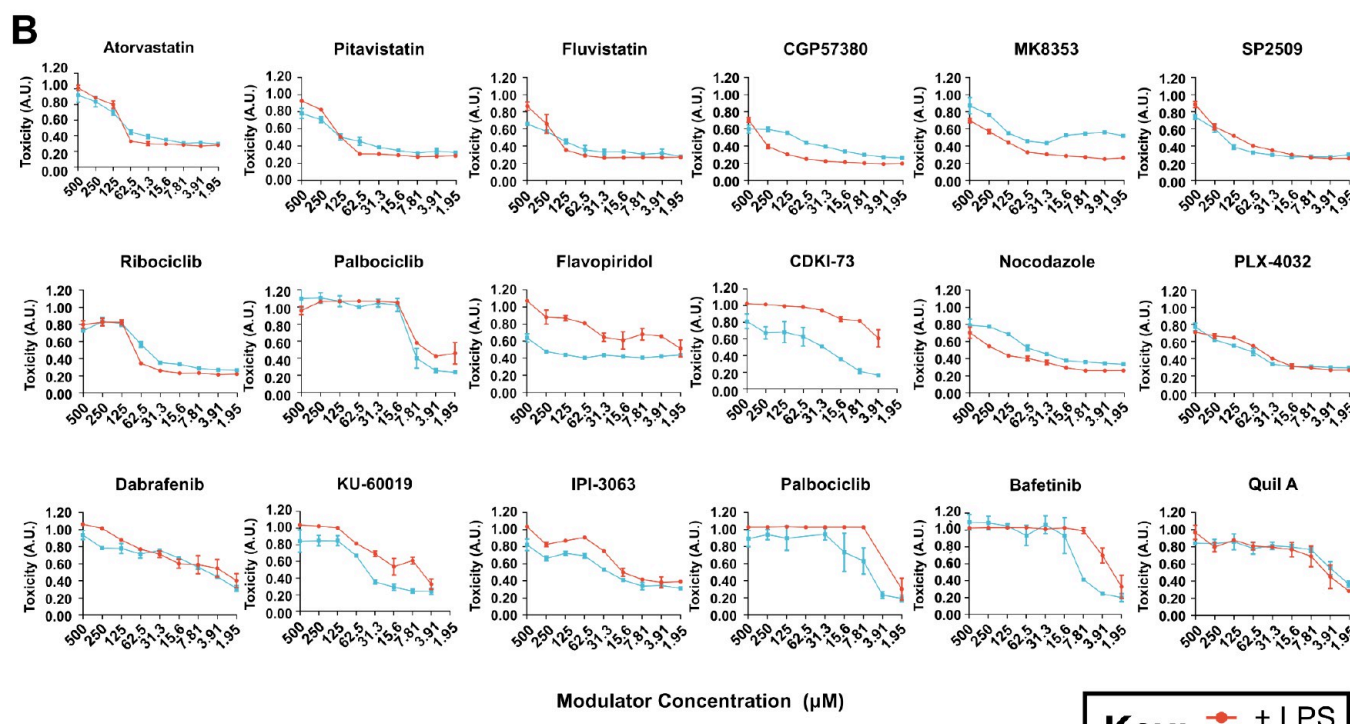
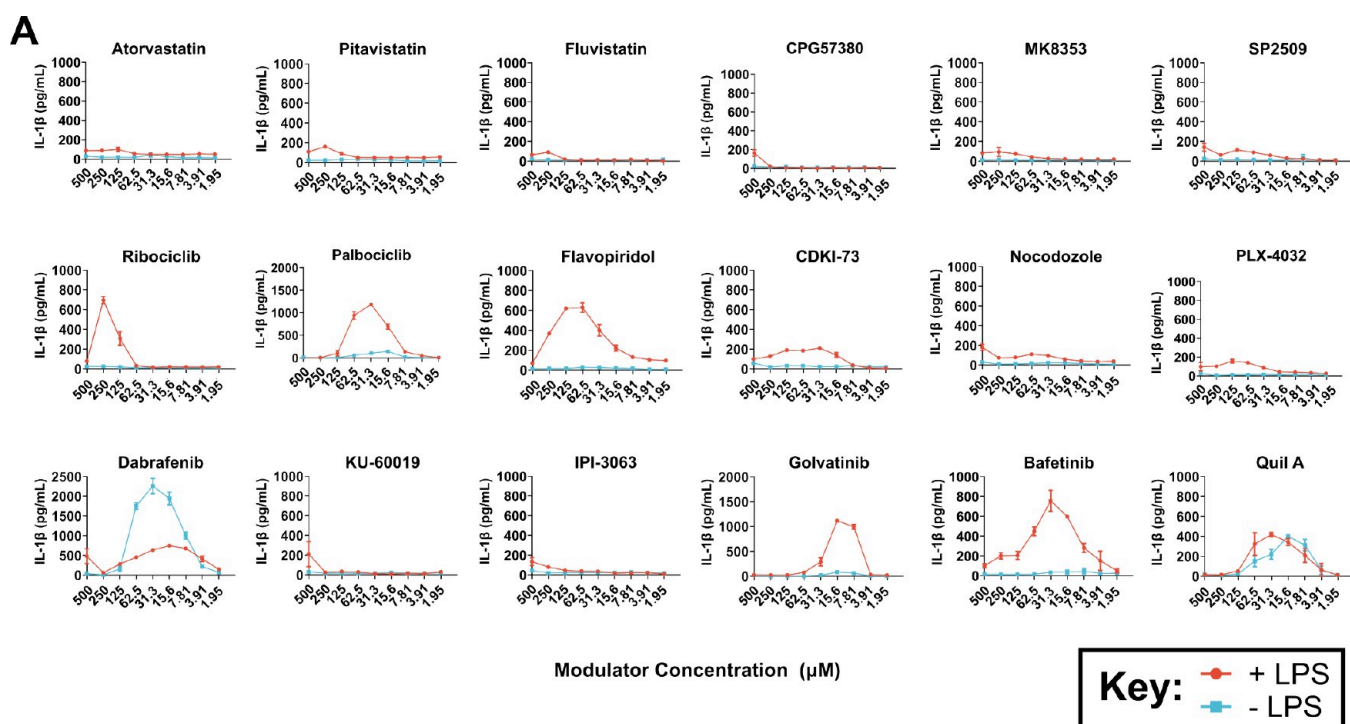


**Figure 1.** (A) IL-1 $\beta$  secretion and (B) toxicity of compounds in BMDMs. LPS-primed or -unprimed BMDMs were treated overnight with the 17 analytes and Quil A as a positive control. IL-1 $\beta$  secretion was assayed using ELISA and quantified using recombinant protein standards. Toxicity was assayed using a secreted lactate dehydrogenase (LDH) assay and quantified as the fraction of positive (nigericin-treated) or negative (untreated) controls (1.0 = 100% LDH release relative to nigericin).

result from this screen was that many of the tested compounds induced high levels of IL-1 $\beta$  secretion when coadministered with LPS (a TLR4 agonist), suggestive of small molecule drug-like

compounds that may activate inflammasomes and serve as alternatives to saponin adjuvants. In this study, we conduct further immunological characterization of these compounds to

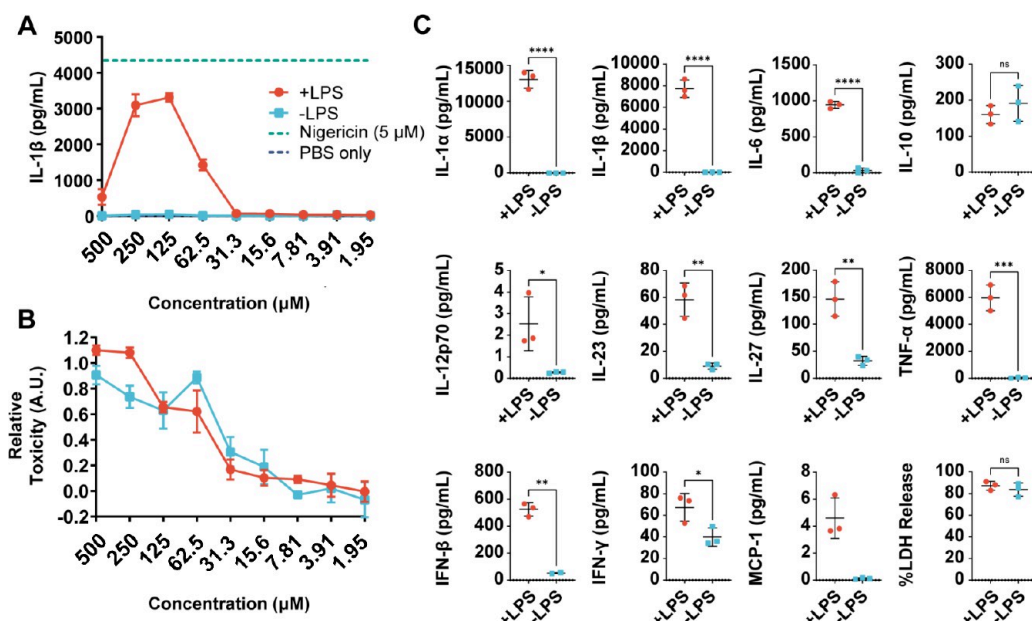


**Figure 2.** Identification of ribociclib as a potent, IL-1 producing adjuvant. (A) IL-1 $\beta$  and (B) LDH release when LPS-primed or -unprimed BMDCs were treated with ribociclib at various concentrations. (C) LPS-primed or -unprimed BMDCs were treated with ribociclib at 125  $\mu$ M, which was found to be a concentration of maximum activity. Cytokine production was assayed using Legendplex Mouse Inflammation 13-plex, and unpaired *t* tests were used to determine differences between groups. IL-17 and GM-CSF are not shown, these cytokines were below the limit of detection for all treatment conditions.

identify and formulate IL-1 $\beta$ -producing small molecules as novel adjuvants. These compounds would have advantages over saponins in terms of scalable synthesis and tunable structures, possibly allowing for the optimization and development of next generation inflammasome activating adjuvants.

## RESULTS AND DISCUSSION

Small molecule immunomodulators that enhance IL-1 $\beta$  secretion in concert with TLR4 agonist signaling are desirable as low-cost and tunable alternatives to saponin adjuvant systems, such as AS01<sub>B</sub>.<sup>16</sup> From our recent high throughput screen, 18 compounds that maximized fold-change increases in IL-1 $\beta$  secretion when administered to LPS-primed THP-1 monocytes were identified (Supporting Information (SI), Table S1).<sup>20</sup> Seven compounds with low solubility or known toxicity concerns were excluded from this initial library, while six additional compounds that target similar signaling pathways as the top-performing compounds were included to obtain a total of 17 initial compounds (SI, Table S1). The compounds selected predominantly included statins, cell cycle modulators, and kinase inhibitors, suggesting similar mechanisms of action. Among these compounds, some had been reported previously to induce IL-1 secretion (see SI, Table S2, for a summary of previous literature), though we did not identify any studies where these compounds were used as vaccine adjuvants.

With a library of 17 candidates in hand, we first validated the activity of these compounds in bone marrow-derived macrophages (BMDMs) derived from C57Bl/6J mice. Macrophages were selected for these pilot studies as they (along with dendritic cells) are key mediators of the innate immune response in vaccination. LPS-primed or -unprimed BMDMs were treated with each compound in serial 2-fold dilutions of 1.9–500  $\mu$ M to identify the concentration where maximum LPS-dependent IL-1 $\beta$  secretion was observed. Toxicity was assayed using secreted lactate dehydrogenase (LDH) relative to the nigericin control

(SI, Figure S1), while IL-1 $\beta$  secretion was assayed using ELISA (Figure 1). Statins identified during the primary screen did not induce high levels of IL-1 $\beta$  secretion in BMDMs, possibly due to cell type or species-specific differences. Others have reported that statins can both induce or inhibit inflammasome activation in a context dependent fashion,<sup>21–23</sup> though further study is warranted. Meanwhile, many of the tested cell cycle modulators and kinase inhibitors resulted in robust LPS priming- and concentration-dependent IL-1 $\beta$  secretion in our treatment regime. Peak IL-1 $\beta$  secretion was concomitant with cell death for all candidate compounds tested, a common feature of inflammasome activation and pyroptotic cell death.<sup>5</sup> One compound, dabrafenib, induced IL-1 $\beta$  secretion independently of LPS priming, a result which has been reported by others<sup>24</sup> and which we hypothesize may result from the activation of alternative caspases and/or signaling pathways outside the scope of this manuscript. We also characterized the production of other pro-inflammatory cytokines when LPS-primed or -unprimed bone marrow-derived dendritic cells (BMDCs) were treated with our candidate compounds at 100  $\mu$ M (SI, Figure S2). For this assay and all subsequent assays, BMDCs were used as an alternative to BMDMs, as they can be isolated in higher yield and were found to exhibit less variability between experiments. 100  $\mu$ M was identified as the concentration of peak activity for many compounds in our preliminary IL-1 $\beta$  screen and used for all compounds in this cytokine panel. Again, many cell cycle modulators and kinase inhibitors induced LPS-dependent secretion of IL-1 $\alpha$ , IL-1 $\beta$ , IL-6, and TNF- $\alpha$ , pro-inflammatory cytokines associated with inflammasome activation and immunogenic cell death.

Based on the results of this initial screen, the Cyclin-Dependent Kinase (CDK) inhibitors, ribociclib, palbociclib, flavopiridol, and CDKI-73, were identified as potent inducers of IL-1 $\beta$  when coadministered with a TLR4 agonist. CDK inhibitors are FDA-approved cancer therapeutics that interrupt cell cycle progression, resulting in senescence and apopto-

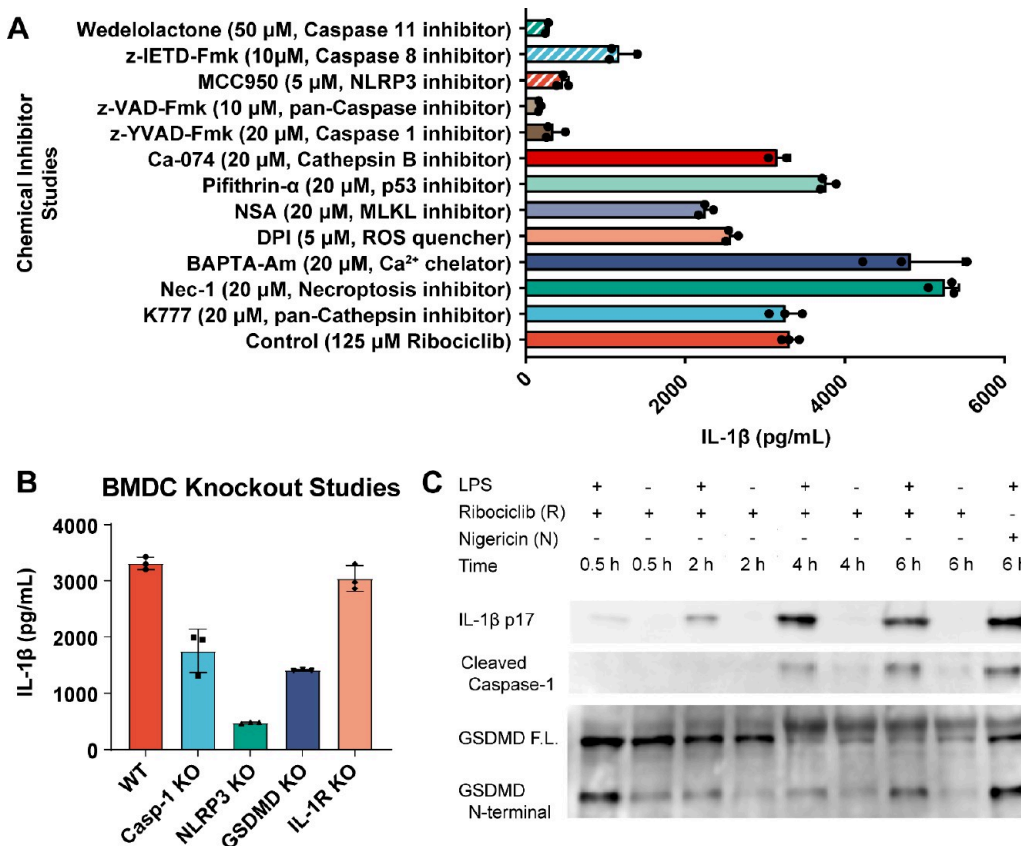


**Figure 3.** Evaluation of ribociclib's mechanism of IL-1 cytokine production. (A) LPS-primed BMDCs were pretreated with the indicated inhibitor compounds for 30 min, then treated with 125  $\mu$ M ribociclib (or 15.6  $\mu$ M, in the case of DPI). IL-1 $\beta$  was measured in the supernatant via ELISA. (B) LPS-primed BMDCs isolated from the indicated KO mice were treated with 125  $\mu$ M ribociclib, and IL-1 $\beta$  was measured in the supernatant via ELISA. (C) LPS-primed or -unprimed BMDCs were treated with 125  $\mu$ M ribociclib or a control, 5  $\mu$ M Nigericin (N), for the indicated time points, then lysed and analyzed via Western blot in the supernatant (S) or lysate (L). Full immunoblots and conditions for antibody staining are provided in SI, Figure S4.

sis.<sup>25–27</sup> In addition to their senescence-inducing properties, CDK inhibitors have been well-reported to induce a Senescence Associated Secretory Phenotype (SASP) characterized by the release of pro-inflammatory cytokines (canonically IL-1 $\alpha$  and IL-6).<sup>28,29</sup> At least one study has shown that SASP-mediated IL-1 secretion is mediated at least partially by inflammasomes.<sup>28</sup> The CDK4/6 inhibitors, palbociclib and ribociclib, have also been reported to enhance CD8+ T cell responses through, as yet, poorly defined mechanisms.<sup>26,30–35</sup> We hypothesized that this immunostimulatory activity could stem partly from the activation of inflammasomes and be enhanced through synergistic codelivery of TLR agonists to facilitate an adjuvant effect. We selected ribociclib for further development as a potential adjuvant candidate. To ensure no differences between our pilot screen in BMDMs and subsequent studies with BMDCs, ribociclib activity was rescreened in LPS-primed or -unprimed BMDCs at 1.9–500  $\mu$ M, and a peak concentration of secreted IL-1 $\beta$  (>3,000 pg/mL) was again observed at 125  $\mu$ M (Figure 2A,B). While cell death was observed in both LPS-unprimed and -primed cells treated with ribociclib, high levels of pro-inflammatory cytokines only occurred with LPS priming (Figure 2C). Finally, ribociclib induced IL-1 $\beta$  secretion in LPS-primed THP-1 human monocytes, though priming with adjuvants targeting other PRRs induced low or undetectable levels of IL-1 $\beta$  secretion (SI, Figure S3). Some studies have reported that other PRRs can serve as a priming signal, though TLR4 agonists are the most potent as they generate unique post-

translational modifications that support NLRP3 inflammasome activation.<sup>36</sup> It is possible that other PRR agonists did not provide a sufficient priming stimulus in this model system to generate detectable levels of IL-1 $\beta$  secretion following treatment with ribociclib. These data encouraged further study into the mechanism of ribociclib-mediated IL-1 $\beta$  secretion.

Having identified ribociclib as a promising target compound, we next probed whether IL-1 $\beta$  secretion resulted from activation of known inflammasome pathways. We first repeated IL-1 $\beta$  secretion studies in BMDCs with various chemical inhibitors. The NLR family pyrin domain-containing protein 3 (NLRP3) inflammasome is the most common and well-studied inflammasome. However, a host of other inflammasomes with similar effector functions and roles in adaptive immunity have been reported.<sup>5</sup> NLRP3 is activated by various signals that disrupt homeostasis, such as lysosomal destabilization, cathepsin release, cellular ion fluxes, or intracellular reactive oxygen, which all result in NLRP3 conformational changes and downstream effector functions.<sup>37</sup> A library of chemical inhibitors blocking various aspects of NLRP3 activation, cell cycle progression, and inflammatory cell death were purchased to probe the mechanism of ribociclib-mediated IL-1 $\beta$  secretion. When BMDCs were pretreated with Ca-074 (a Cathepsin B inhibitor), DPI (a reactive oxygen quencher), NSA (a MLKL inhibitor), K777 (a pan-Cathepsin inhibitor), or Pifithrin- $\alpha$  (a p53 inhibitor) before the addition of our target compounds, few changes in IL-1 $\beta$  secretion were observed, indicating that the

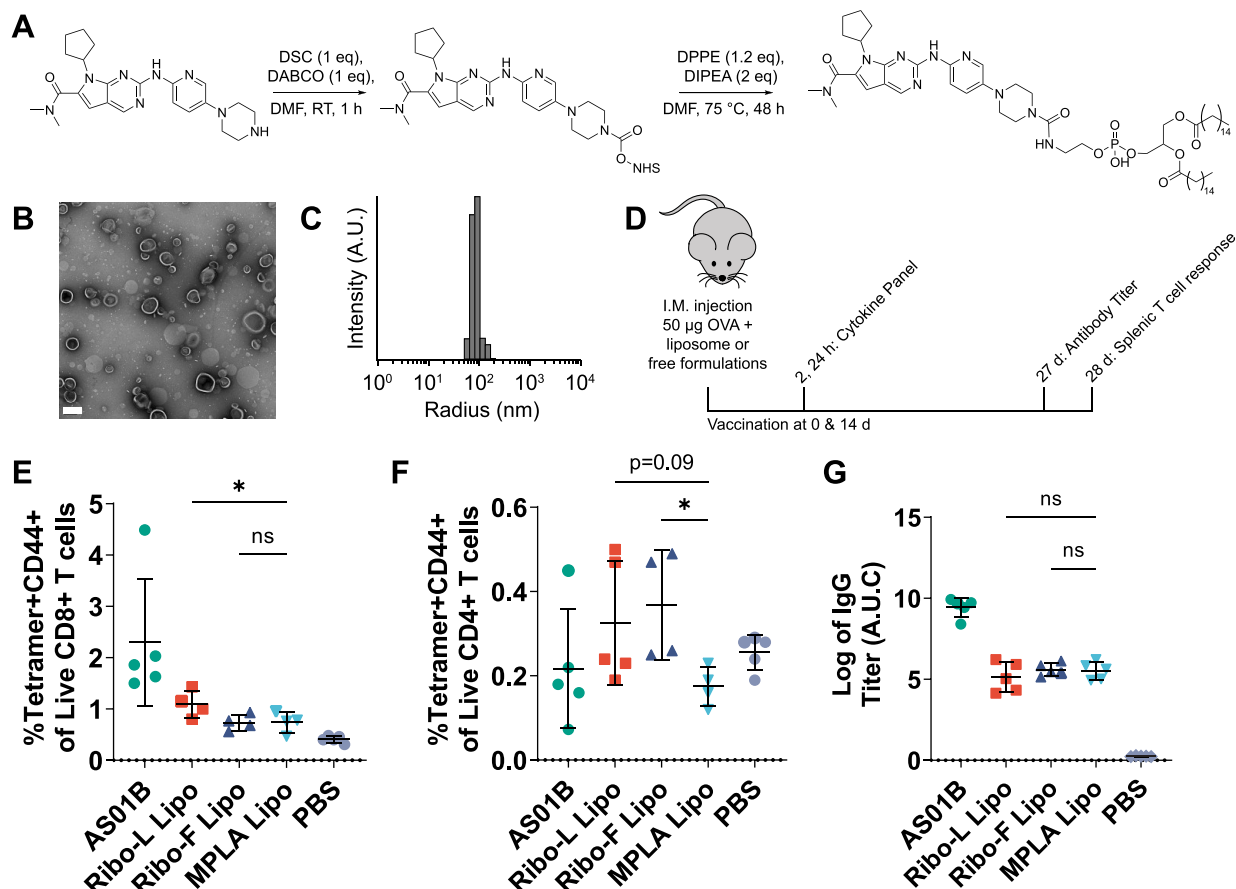


**Figure 4.** Synthesis, formulation, and *in vivo* responses of ribociclib lipid derivatives. (A) Synthetic scheme for the preparation of Ribo-L in two steps from commercially available ribociclib. (B) TEM image of Ribo-L formulated at 40  $\mu$ g/mL within DSPC and MPLA containing liposomes (scale bar = 250 nm). (C) Representative DLS of monodisperse liposome formulation. (D) Vaccination schedule for the characterization of ribociclib-containing formulations *in vivo*. (E) Splenic, antigen specific CD8+ and (F) CD4+ T cell responses 28 d after vaccination. (G) Anti-OVA IgG titer 27 d after initial vaccination.

inhibited components of inflammasome machinery do not play a role in ribociclib-mediated IL-1 $\beta$  secretion (Figure 3A). In contrast, treatment with direct inhibitors of NLRP3 or caspases -1, -8, and -11 dramatically reduced IL-1 $\beta$  secretion, suggesting that ribociclib activates inflammasomes downstream of these common signaling modalities (Figure 3A). Finally, treatment with BAPTA-AM (a calcium chelator) or Nec-1 (a necroptosis inhibitor) surprisingly increased IL-1 $\beta$  secretion relative to the control, indicating that these compounds do not block ribociclib-mediated IL-1 $\beta$  secretion but may prolong the duration of secretion prior to cell death (Figure 3A). To query the role of NLRP3 more definitively, we repeated assays in BMDC-KOs lacking components of inflammasome machinery: NLRP3, caspase-1 (Casp1), and gasdermin D (GSDMD) (Figure 3B). Knockout of these inflammasome components reduced IL-1 $\beta$  secretion, though 10–50% of the measured IL-1 $\beta$  was still observed depending on the knocked-out component, suggesting a partial role for a second, contributing cell death pathway. In contrast, knocking out IL-1R as a control treatment did not affect IL-1 $\beta$  secretion, as these cells should secrete comparable levels of IL-1 $\beta$  as wild-type mice despite their lack of a cognate receptor (Figure 3B). Finally, we conducted Western blot studies to directly confirm LPS-dependent activation of inflammasomes by ribociclib in BMDCs. Western blots of lysates and supernatants for cleavage products of active inflammasome machinery show that treatment with ribociclib

induced active Casp1 production followed by cleavage of GSDMD and IL-1 $\beta$  to their active form after 2–4 h (Figure 3C, and SI, Figure S4). Additional Western blots for phosphorylated MLKL (a marker of necroptosis)<sup>38</sup> or phosphorylated Rb protein (a protein which is inhibited during CDK-induced senescence)<sup>34</sup> were negative and did not indicate activation of alternative cell death pathways. These data, in total, provide evidence that ribociclib and other CDK4/6 inhibitors activate inflammasomes to mediate IL-1 $\beta$  secretion. We hypothesize that CDK4/6 inhibitors may activate inflammasomes and generate IL-1 responses by inducing DNA damage responses and activation of pro-inflammatory transcriptional programs (such as NF- $\kappa$ B) associated with senescence,<sup>39</sup> though further work beyond the scope of this study is needed to validate this hypothesis.

Having generated strong evidence of inflammasome activation *in vitro*, ribociclib was formulated for vaccination in C57Bl/6J mice using a prophylactic ovalbumin (OVA) model. As inflammasome-activating adjuvants typically require both a TLR agonist signal and an activating signal, ribociclib (50 nmol/dose) was codelivered with a TLR4 agonist, MPLA (5  $\mu$ g/dose), which has improved safety relative to LPS and is approved for use in humans.<sup>12,40</sup> A saponin adjuvant, Quil-A, that is related to the QS-21 component of GSK's AS01 formulation,<sup>16</sup> was similarly coformulated with MPLA and used as a best-in-class benchmark standard. In a pilot study, the indicated adjuvant

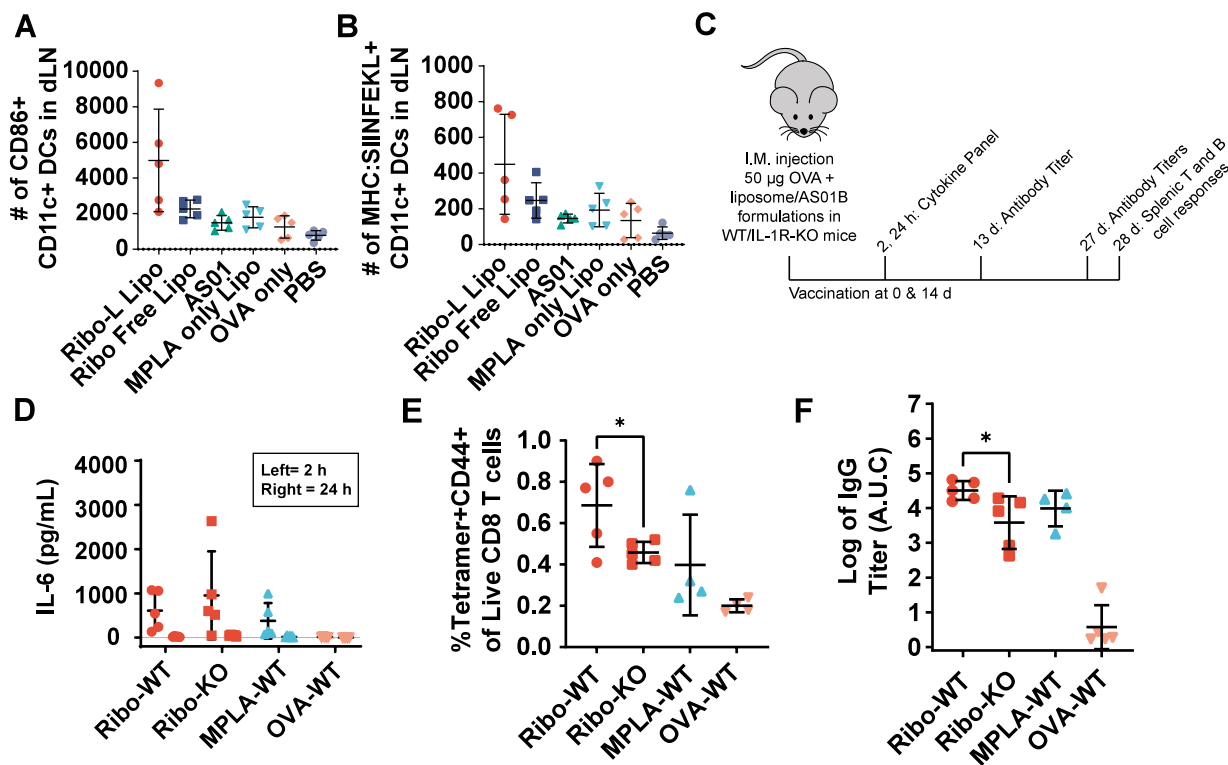


**Figure 5.** *In vivo* mechanism of ribociclib-mediated immunity. (A) Upregulation of the cell surface marker, CD86, and (B) enhanced presentation of MHC-I restricted antigen on dendritic cells in the draining inguinal lymph node of mice injected intramuscularly with the indicated formulations. (C) Vaccination schedule for a comparative study between wild-type (WT) and IL-1R deficient (KO) C57Bl/6J mice. (D) Systemic IL-6 in the serum of WT or KO mice vaccinated with the indicated formulations after 2 or 24 h. (E) Splenic, antigen-specific CD8<sup>+</sup> T cell responses. (F) Total IgG titers generated in response to the indicated formulations. One-way ANOVA with Sidak's multiple comparisons test is shown in E-F.

formulations were injected intramuscularly with 50  $\mu$ g OVA, mice were boosted at day 13, and experiments were terminated at day 26 (SI, Figure S5A). Here, ribociclib-adjuvanted vaccines enhanced early IFN- $\gamma$  production at 24 h relative to Quil-A, though IL-6 and MCP-1 levels were reduced relative to Quil-A (SI, Figure S5B). Evaluation of the adaptive response revealed that ribociclib induced minor increases in OVA-specific antibody and CD8<sup>+</sup> T cell responses relative to MPLA alone (SI, Figure S5C–E). In a follow-up study, ribociclib formulations containing 10, 100, or 1000 nmol/dose were employed (SI, Figure S6). Here, ribociclib induced a modest increase in splenic, antigen specific CD8<sup>+</sup> T cell production at 10 and 100 nmol relative to MPLA alone. In both studies, the adaptive immune response paled in comparison to an AS01-like formulation containing Quil-A and MPLA, suggesting a need for formulation optimization. To this end, we hypothesized that the high bioavailability of ribociclib, which was originally synthesized as an orally available drug, resulted in poor retention at the injection site. This would limit its immunogenic effects during intramuscular injection. With this limitation in mind, we sought to improve the formulation of ribociclib for vaccination by encapsulating it into liposomes.

Liposomal formulations have become common tools to modify the physicochemical properties of active pharmaceutical ingredients (APIs) and control their delivery to specific cell and organelle subsets. In liposomes, hydrophilic APIs can be loaded into the aqueous core or lipid bilayer of the lipid-based nanoparticle. The resulting nanoparticles have desirable size and physicochemical properties for endocytosis and delivery to the endosome, where they can activate endo/lysosomal receptors to facilitate a desired response—in the case of vaccination,

immunogenic cytokine release.<sup>41</sup> Still, poor loading of aqueous APIs hinders control over the loading and delivery of large quantities of payload.<sup>42</sup> To better control the loading and delivery of ribociclib to the endosomal compartment of antigen presenting cells, where it could activate inflammasomes and initiate targeted IL-1 $\beta$  secretion, a lipid-modified version of ribociclib containing a 1,2-dipalmitoyl-sn-glycero-3-phosphoethanolamine (DPPE) tail was prepared from ribociclib in two steps (Ribo-L, Figure 4A, and SI, Figure S7). DPPE may be cleaved by lysosomal phospholipases<sup>43</sup> to release ribociclib with a four-atom modification at the piperazine terminus, a site amenable to modification in previous structure–activity studies.<sup>44</sup> Lipid functionalization reduced IL-1 $\beta$  secretion from ~3000 pg/mL to ~1000 pg/mL at 125  $\mu$ M (SI, Figure S8). It was reasoned that the enhanced delivery of Ribo-L would benefit *in vivo* delivery despite the reduction in activity *in vitro*. Future efforts will focus on the structure activity relationship of Ribo-L derivatives. Ribo-L was then incorporated alongside MPLA into 1,2-distearoyl-sn-glycero-3-phosphatidylcholine (DSPC)-comprised liposomes, prepared via thin film rehydration and extrusion through a 200 nm filter.<sup>42</sup> Liposomes loaded with 40, 200, or 1,000  $\mu$ g/mL of Ribo-L and 100  $\mu$ g/mL MPLA were found to have similar size, charge, and shape as MPLA-only control liposomes as well as high loading efficiencies (Figure 4B,C, and SI, Figures S9–S12), demonstrating successful implementation of this formulation strategy.

Having successfully prepared Ribo-L loaded liposomes, prime-boost vaccination studies were repeated to evaluate if these formulations could enhance vaccine efficacy relative to soluble formulations. Liposomes prepared with 200  $\mu$ g/mL of Ribo-L or free ribociclib (Ribo-F) and 10  $\mu$ g/mL MPLA were

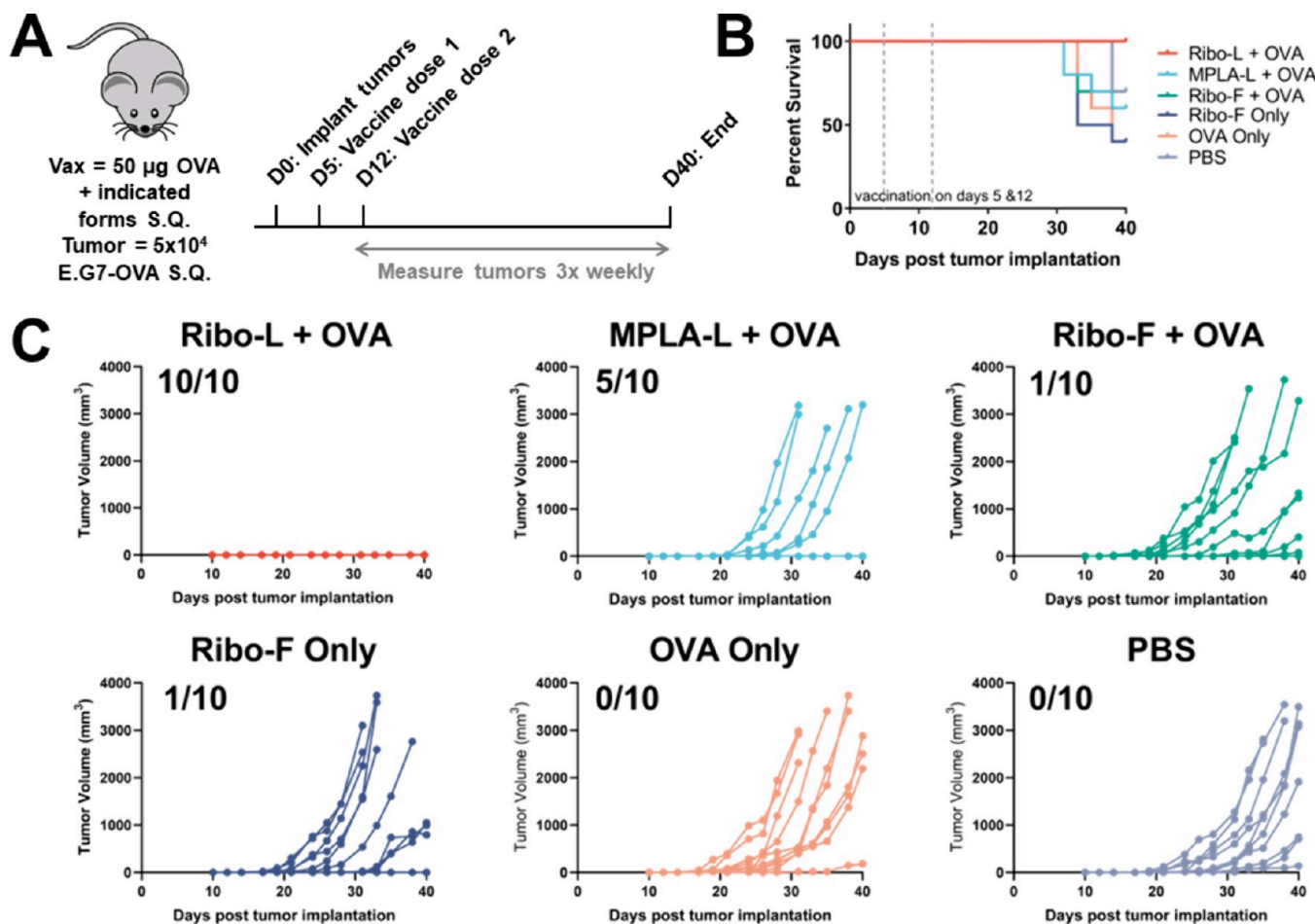


**Figure 6.** *In vivo* tumor therapeutic vaccination study of Ribo-L containing liposomes and controls. (A) Vaccination schedule for the tumor challenge model ( $n = 10$ /group). Mice were implanted with  $5 \times 10^4$  E.G7-OVA cells subcutaneously. They were vaccinated 5 and 12 d after tumor implantation with the indicated formulations peritumorally. Tumor growth and survival were monitored 3 times/week until day 40. (B) Kaplan–Meier curve showing survival of mice treated with various formulations throughout the study. (C) Tumor growth curves of individual mice treated with each of the formulations.

used for vaccination as shown in Figure 4. AS01<sub>B</sub>, which is an FDA approved adjuvant comprised of a Quil-A isolate, QS-21, and MPLA coformulated in liposomes, was used as a positive control in these studies. Mice vaccinated with the liposomes containing a reduced MPLA dose and Ribo-L or Ribo-F did not show differences in systemic cytokine release relative to MPLA only at 2 or 24 h after injection (SI, Figure S13). The Ribo-L and Ribo-F liposomes, however, did afford a statistically significant increase in splenic, antigen-specific CD4+ and CD8+ T cell responses relative to MPLA-only liposomes as measured by tetramer staining (Figure 4E,F, and SI, Figure S14). No differences in the antibody response were observed (Figure 4G). Both antibody and T cell responses were inferior to AS01<sub>B</sub>, highlighting the desirability of further optimizing this platform. Nevertheless, these data supported our hypothesis that ribociclib enhances adaptive immune responses in vaccination.

Having successfully developed a ribociclib-containing formulation for vaccination, further efforts were undertaken to understand the behavior of Ribo-L liposomes *in vivo*. First, we asked whether these liposomes enhance the activation of dendritic cells in the draining lymph node. Mice were injected with vaccines containing OVA formulated with liposomal or free ribociclib, AS01<sub>B</sub>, or PBS, and the draining inguinal lymph node was dissected 5 d later (modeling a study by Li et al.<sup>45</sup>) for

immunophenotypic analysis. Ribo-L containing liposomes upregulated surface expression of CD86 and MHC-I on dendritic cells in the draining lymph node (Figure 5A,B). This phenotype is indicative of dendritic cell activation and antigen presentation, both hallmarks of a productive innate immune response. We then asked whether adjuvant effects generated from Ribo-L formulations were dependent on IL-1 receptor (IL-1R) signaling *in vivo* (analogous to the *in vitro* data presented in Figure 3). IL-1R-deficient mice or wild-type (WT) controls were vaccinated with OVA-containing Ribo-L liposomes, MPLA-only liposomes, or a control PBS formulation (Figure 5C). No difference in systemic IL-6 production was observed between IL-1R-deficient and WT mice after treatment with Ribo-L liposomes at 2 or 24 h after injection (Figure 5D). Despite this lack of early cytokine response, IL-1R-deficient mice had reduced OVA-specific CD8+ T cell responses relative to their WT counterparts after treatment with Ribo-L liposome adjuvanted vaccines (Figure 5E). Moreover, IL-1R-deficient mice had reduced anti-OVA IgG responses after treatment with Ribo-L liposomes (Figure 5F, and SI, Figure S15). While total IgG and CD8+ T cell responses were reduced in IL-1R-KO mice, these changes did not correspond with differences in the IgG2c/IgG1 ratio, a feature often associated with T<sub>H</sub>1-biased responses (SI, Figure S14). Altogether, these results support the

hypothesis that Ribo-L liposomes induce IL-1 cytokine release in the draining lymph node to facilitate upregulation of cell surface markers and enhanced antigen presentation.

We next asked whether the ribociclib-containing liposomes could generate an adjuvant effect in a therapeutic cancer model. Ribociclib is an approved chemotherapy for estrogen receptor positive (ER+) human epidermal growth factor receptor 2 negative (HER2-) breast cancer, though for its approved indication, it is used orally at a high dose in combination with an aromatase inhibitor.<sup>46</sup> Our studies show that ribociclib synergizes with a TLR4 agonist at much lower doses in a liposomal formulation to induce an immunostimulatory environment characterized by inflammasome activation, IL-1 $\beta$  secretion, and enhanced CD8+ T cell responses. Given that pro-inflammatory cytokine production and CD8+ T cell biasing are key facets of anticancer immunity,<sup>47</sup> we hypothesized that peritumoral, subcutaneous administration of ribociclib-containing liposomes with a tumor antigen could generate an adjuvant effect and aid in tumor clearance. To address this hypothesis, an E.G7-OVA lymphoma model was employed. The  $5 \times 10^4$  tumor cells were implanted into the right flank of C57B1/6J mice ( $n = 10$ /group) on day 0. Mice were vaccinated subcutaneously on days 5 and 12 postimplantation with vaccine formulations containing 50 nmol Ribo-L + 5  $\mu$ g MPLA in liposomes with 50  $\mu$ g OVA, MPLA-only liposomes (MPLA-L) with OVA, free ribociclib (50 nmol) with or without OVA, or controls (Figure 6A). Mice were monitored for tumor growth 3X weekly through day 40 and sacrificed when tumor size reached 20 mm in any linear dimension. It was found that Ribo-L liposome vaccine treatments led to complete remission of tumors in treated animals on day 40 (Figure 6B,C). In contrast, mice treated with MPLA-only liposomes led to remission in 50% of treated animals, and other treatment groups, by and large, failed to suppress tumor growth (Figure 6B,C). This result confirms that Ribo-L liposomes induce a robust, antigen-specific adjuvant effect when used for therapeutic vaccination. More broadly, it highlights that ribociclib-containing formulations could hold potential for cancer immunotherapy driven by high IL-1 cytokine release and potent CD8+ T cell responses. While further studies are needed to fully elucidate the mechanism behind the adjuvant effect of ribociclib and optimize its structure for broader clinical implementation, this study provides proof of principle supporting the use of CDK inhibitors as novel adjuvants for both prophylactic and therapeutic vaccine indications.

## CONCLUSION

In this study, we report the identification of a small molecule CDK4/6 inhibitor, ribociclib, as a novel inflammasome activating adjuvants for vaccination. Ribociclib induced IL-1 $\beta$  secretion in LPS-primed dendritic cells and macrophages. IL-1 $\beta$  release was found to be caspase-, NLRP3-, and GSDMD-dependent through both inhibitor and knockout studies. When coformulated in liposomes with a TLR4 agonist, MPLA, and used for vaccination with a model antigen, OVA, ribociclib generated enhanced antigen specific CD4+ and CD8+ T cell responses relative to controls. Ribociclib also enhanced T cell and antibody responses dependent, partially, upon IL-1R signaling. While further work is needed to uncover the mechanism of CDK4/6 inhibitor mediated inflammasome activation, these compounds could serve as low-cost, tunable adjuvant platforms for use in vaccination and cancer immunotherapy. More globally, these results highlight the

potential of using new small molecules and stimulating alternative signaling pathways to generate IL-1 mediated adjuvant effects in vaccination.

Several studies have identified that ribociclib and other CDK inhibitors enhance cell-mediated adaptive immune responses when used to induce cell cycle arrest in the context of cancer therapy.<sup>30–33</sup> In this study, we report inflammasome activation as an additional immune-potentiating effect of ribociclib. CDK inhibitors have long been reported to induce high levels of pro-inflammatory cytokine production via the SASP. This work suggests that there is the potential that these cytokines are also induced, at least in part, from the activation of inflammasomes by ribociclib.<sup>28</sup> Co-administration of ribociclib with TLR4 agonists was shown to bolster IL-1 secretion through caspase-dependent mechanisms *in vitro* and enhance antigen presentation *in vivo*. Moreover, CD8+ T cell responses were enhanced after prime-boost vaccination when ribociclib was formulated into liposomes. Enhanced CD8+ and T<sub>H</sub>1 responses are a key feature of some NLRP3 ligands,<sup>10</sup> though correlating inflammasome activation to the adjuvant activity of vaccine formulations has proven challenging.<sup>2</sup> The data herein provides preliminary evidence that treatment of ER+HER2- patients with ribociclib could facilitate an adjuvant effect during breast cancer therapy by activating inflammasomes, in addition to its known functions.

This work does not provide conclusive evidence of the mechanistic connection between CDK4/6 and inflammasome activation. Genetic ablation of the interaction between CDK4/6 and Cyclin D is embryonic lethal.<sup>48,49</sup> Inflammasome activation results in pyroptosis, a rapid and inflammatory mode of cell death, rendering difficult many of the kinase-dependent or -independent experiments used traditionally. While we provide evidence suggesting caspase and NLRP3 inhibition by ribociclib, future work must be conducted to understand how these compounds mediate this phenotype. Kinase screening in parallel with proteomics and transient genetic knockdowns could provide critical information toward achieving this goal, though these assays are well beyond the scope of this early work. Moreover, it must be noted that knockout of key inflammasome machinery does not completely abrogate secretion of IL-1 $\beta$  after treatment with ribociclib (Figure 3B), and pretreatment with Wedelolactone or z-IETD-fmk (caspase-11 and caspase-8 inhibitors, respectively) dramatically reduced IL-1 $\beta$  secretion (Figure 3A). Together, these results suggest that multiple caspases and/or inflammasome pathways may be activated by ribociclib, though further mechanistic work is needed to validate these preliminary data.

This study supports the identification of novel small molecule adjuvants targeting the NLRP3 inflammasome and/or IL-1 $\beta$  secretion for use in vaccination. Many FDA-approved vaccine APIs have been shown in recent years to activate inflammasomes, including saponins and the ionizable lipid component of mRNA lipid nanoparticles.<sup>2,3,50</sup> While these APIs are very successful in vaccination, they can be challenging and expensive to prepare, and they induce reactogenicity in many individuals—limiting wider adoption of these platforms. Small molecules, on the other hand, are often less costly and more easily tunable. Developing small molecule inflammasome activators would allow for better control over inflammasome activation, induce safer and/or more efficacious responses, and improve vaccine accessibility to a larger population. Ribociclib can be prepared on an industrial scale in 5–6 synthetic steps,<sup>51</sup> and the lipid modification reported herein requires only two additional steps.

While more work will be needed to optimize the structure and demonstrate improvements in reactogenicity of Ribo-L and analogue compounds relative to saponin adjuvants, this study provides evidence that these compounds generate robust IL-1 $\beta$  secretion and T cell responses. This insight will both expand the scope of use for ribociclib to vaccination.

## MATERIALS AND METHODS

**Mice and Materials.** All chemicals and cell culture reagents were obtained from Sigma-Aldrich or Thermo Fisher and used without further purification unless otherwise noted. SI, Table S3 provides the vendors and product codes of screening compounds and inhibitors. For synthesis, ribociclib was purchased from AmBeed, and N,N'-disuccinimidyl carbonate was purchased from AA Blocks. Lipid reagents for liposomes (including synthetic MPLA-PHAD) were purchased from Avanti Polar Lipids. A table providing the clone and source of all antibodies used for flow cytometry and Western blots is provided in SI, Table S4. The human Shingrix vaccine was purchased from VaccineShoppe through an approved contract with the IIT Research Institute that allows for animal use. For *in vitro* assays, cells were maintained at 37 °C and 5% CO<sub>2</sub>. For *in vivo* studies, female, 6-week-old C57Bl6/J (WT), B6.129S6-Nlrlp3tm1Bhk/J (NLRP3-KO), B6N.129S2-Casp1tm1Flv/J (Casp1-KO), C57BL/6J-Gsdmdem1Vnce/J (GSDMD-KO), and B6.129S7-II1r1tm1Imx/J (IL-1R-KO) were purchased from Jackson Laboratories and allowed to acclimate for at least 1 week before use. Mice were housed in an AAALAC-accredited animal facility with controlled light, temperature, and humidity conditions and supplied with food and water ad libitum. All animal procedures were performed under a protocol approved by the University of Chicago Institutional Animal Care and Use Committee. Unless otherwise noted, all data are analyzed and plotted in GraphPad Prism 9. All synthesized compounds are >95% pure by HPLC analysis. The authors identify no unexpected, new, or significant hazards or risks associated with the compounds used in this work.

**Selection and Preparation of Hit Compounds.** The high throughput screen was conducted as reported in M.G. Rosenberger, J.Y. Kim et al.<sup>20</sup> using automated high throughput instrumentation as described in the Supporting Information. Hit compounds for secondary screening were selected by evaluating the fold-change increase in IL-1 $\beta$  secretion in THP-1 cells treated with LPS-EK (100 nM, InvivoGen) with modulators relative to LPS-EK alone (SI, Table S1). Compounds with solubility <10 mM in DMSO were excluded. Palbociclib, flavopiridol, CDK1-73, dabrafenib, bafetinib, and IPI-3063 were also included in the screen based on preliminary data suggesting high levels of activity, while Quil-A was included as a control with known activity *in vivo*. For all *in vitro* studies, 10 mM solutions of the inhibitors were prepared in DMSO and diluted in PBS to 10x the working concentration before addition to cells.

**IL-1 $\beta$ , LDH, and Other Cytokine Secretion in Primary Murine Cells.** Bone-marrow derived macrophages (BMDMs) or dendritic cells (BMDCs) from wild-type or indicated knockout mice were isolated and differentiated as reported previously.<sup>52,53</sup> After 6 d of differentiation, cells were mechanically detached, washed, and plated in a 96-well plate at 1.8 × 10<sup>5</sup> cells/well in 180  $\mu$ L fresh medium (RPMI + 10% HI-FBS). Cells were allowed to adhere for 1 h and then treated with 20  $\mu$ L of 10× ultrapure LPS-EB (working concentration 100 EU/mL) or PBS. After 3 h, cells were washed and resuspended in 180  $\mu$ L fresh medium. Where relevant, cells were pretreated with inhibitors (2  $\mu$ L of 100× working concentration in DMSO as noted in the figures) for 30 min. Then 20  $\mu$ L of 10× hit compounds were added and incubated overnight. After 16 h, the supernatant was collected and subjected to CyQUANT LDH Cytotoxicity Assay (Thermo Scientific) and ELISA MAX Mouse IL-1 $\beta$  Assay (BioLegend) according to the manufacturer's procedures. Absorbance readouts were collected using a Multiskan FC plate reader (Thermo Scientific). For analysis of additional cytokines, an analogous procedure was employed, and supernatant was analyzed using LEGENDplex Mouse Inflammation 13-plex (BioLegend) according to the manufacturer's procedure. Multiplex data was collected using a Novocyte ACEA flow cytometer (Agilent).

**Immunoblot Assays.** BMDCs were isolated and cultured as described above and plated in untreated 24 well plates at 1 × 10<sup>6</sup> cells/well. Cells were treated with 100 EU/mL ultrapure LPS-EB (InvivoGen) or PBS for 3 h, then washed and treated with ribociclib (100  $\mu$ M) or nigericin (5  $\mu$ M) for the indicated times. The supernatant was then collected, and cells were lysed with 200  $\mu$ L M-PER (Thermo Scientific) containing 1× Protease/phosphatase Inhibitor Cocktail (Cell Signaling Technologies). Reducing, denaturing SDS-PAGE gel chromatography was then conducted using 12% Mini-PROTEAN TGX Precast Gels (BioRad). Blots were transferred to PVDF membranes using a Trans-Blot turbo transfer system (BioRad). Membranes were blocked with TBS-T + 5% nonfat milk at room temperature (RT) for 1 h, washed 3 × 5 min with TBS-T, then stained with the indicated antibodies (SI, Table S4) in TBS-T + 1% BSA overnight at 4 °C. After 16 h, membranes were washed 3 × 5 min with TBS-T and stained with HRP Goat anti-Rabbit or Goat anti-Mouse IgG (Thermo Scientific) in TBS-T + 1% BSA at RT for 1 h in the dark. Finally, membranes were washed 5 × 5 min with TBS-T, treated for 10 min with Supersignal West Dura Extended Duration Chemiluminescent Substrate (Thermo Scientific), and imaged using an Azure 600 imager (Azure Biosystems). Images were processed using FIJI for ImageJ.

**Vaccination Studies.** Age-matched, 6-to-12-week-old female C57Bl/6J mice were vaccinated intramuscularly in the flank with 50  $\mu$ L of vaccine formulations. For soluble formulations, vaccines were prepared in 7:2:1 PBS:PEG300:DMSO and filtered through a 200 nm sterile filter before injection. For liposomal formulations, dialyzed liposomes were added to lyophilized antigens and briefly vortexed before injection to mimic GSK's Adjuvant System formulations.<sup>54</sup> Unless otherwise noted, studies with OVA contained 50  $\mu$ g OVA, 10  $\mu$ g VacciGrade sMPLA (InvivoGen), and 50 nmol of modulators (SelleckChem) or 10  $\mu$ g Quil-A (InvivoGen), while liposomes contained 50  $\mu$ g OVA, 5  $\mu$ g sMPLA (Avanti Polar Lipids), and 10 nmol of Ribo-L. The synthesis of Ribo-L and preparation of liposomal formulations are described in the Supporting Information. Where noted, AS01<sub>B</sub> was obtained from the Shingrix vaccine and used at 1/10th of the human dose. Mice were vaccinated at experiment onset and again on day 14. Two and 24 h after the initial injection, serum was collected and assayed for cytokine release using LEGENDplex Mouse Inflammation 13-plex (BioLegend) according to the manufacturer's protocol on a Novocyte ACEA flow cytometer (Agilent). On days 13 and 27, mice were bled via the submandibular vein for antibody titers. On day 28, mice were sacrificed, and spleens were harvested for flow cytometry and/or restimulation. Antibody titer and T cell assays are described in the Supporting Information.

**Antigen Presentation Studies.** Age-matched, 6- to 12-week-old female C57Bl/6J mice were vaccinated intramuscularly in the flank with 50  $\mu$ L of vaccine formulations as described above. After 5 d, the ipsilateral inguinal draining lymph node was collected and enzymatically digested with collagenase (1 mg/mL) and DNase (100  $\mu$ g/mL) at 37 °C for 1 h. Digested lymphocytes were passed through a 40  $\mu$ m cell strainer, pelleted, and resuspended in 200  $\mu$ L PBS. Cells were stained for viability and cell surface markers (SI, Table S4) and analyzed with a Novocyte Penteon (Agilent) flow cytometer. Flow cytometry data was analyzed using FlowJo v10.8.1.

**Tumor Challenge Studies.** Age-matched, 6-to-12-week-old female C57Bl/6J mice were injected subcutaneously on the right flank with 5 × 10<sup>4</sup> EG7-OVA cells in 100  $\mu$ L of PBS at experiment onset. Mice were anesthetized with isoflurane and shaved at the site of the tumor injection before tumor implantation. Mice were then injected subcutaneously on days 5 and 12 post-tumor inoculation with vaccines. The control group received PBS. For soluble formulations, vaccines were prepared in 7:2:1 PBS:PEG300:DMSO and filtered through a 200 nm sterile filter before injection. Dialyzed liposomes were added to lyophilized antigens for liposomal formulations and briefly vortexed before injection. Unless otherwise noted, all formulations contained 50  $\mu$ g OVA, 5  $\mu$ g VacciGrade sMPLA (InvivoGen), and 50 nmol of ribociclib, while liposomes contained 50  $\mu$ g OVA, 5  $\mu$ g sMPLA (Avanti Polar Lipids), and 10 nmol of Ribo-L. The tumor size was monitored thrice weekly starting on 10 d. Tumor volumes were measured using the

equation  $V = 1/2 \times L \times W \times W$ , where  $L$  represents the longer measured dimension and  $W$  represents the shorter measured dimension. Mice were sacrificed when the tumors reached 20 mm in any linear dimension or if signs of distress were observed. On day 40, the remaining mice were sacrificed.

## ■ ASSOCIATED CONTENT

### SI Supporting Information

The Supporting Information is available free of charge at <https://pubs.acs.org/doi/10.1021/acs.jmedchem.4c00516>.

Additional methods, preliminary *in vitro* screening data, full unprocessed Western blots, preliminary *in vivo* vaccination studies with unmodified ribociclib, synthetic details, and NMR spectra for Ribo-L, *in vitro* IL-1 $\beta$  release generated by Ribo-L, characterization of liposomes, additional *in vivo* readouts and supporting data for Ribo-L vaccination studies, lists of vendors (and clones, where relevant) for all antibodies and small molecule inhibitors used ([PDF](#))

SMILES string computer-readable identifiers for the presented molecules ([CSV](#))

## ■ AUTHOR INFORMATION

### Corresponding Author

**Aaron P. Esser-Kahn** — Pritzker School of Molecular Engineering, University of Chicago, Chicago, Illinois 60637, United States;  [orcid.org/0000-0003-1273-0951](https://orcid.org/0000-0003-1273-0951); Email: [aesserkahn@uchicago.edu](mailto:aesserkahn@uchicago.edu)

### Authors

**Adam M. Weiss** — Pritzker School of Molecular Engineering, University of Chicago, Chicago, Illinois 60637, United States; Department of Chemistry, University of Chicago, Chicago, Illinois 60637, United States;  [orcid.org/0000-0002-4972-1402](https://orcid.org/0000-0002-4972-1402)

**Marcos A. Lopez II** — Pritzker School of Molecular Engineering, University of Chicago, Chicago, Illinois 60637, United States; Department of Chemistry, University of Chicago, Chicago, Illinois 60637, United States

**Matthew G. Rosenberger** — Pritzker School of Molecular Engineering, University of Chicago, Chicago, Illinois 60637, United States

**Jeremiah Y. Kim** — Pritzker School of Molecular Engineering, University of Chicago, Chicago, Illinois 60637, United States

**Jingjing Shen** — Pritzker School of Molecular Engineering, University of Chicago, Chicago, Illinois 60637, United States

**Qing Chen** — Pritzker School of Molecular Engineering, University of Chicago, Chicago, Illinois 60637, United States

**Trevor Ung** — Pritzker School of Molecular Engineering, University of Chicago, Chicago, Illinois 60637, United States

**Udoka M. Ibeh** — Pritzker School of Molecular Engineering, University of Chicago, Chicago, Illinois 60637, United States; Pritzker School of Medicine, University of Chicago, Chicago, Illinois 60637, United States

**Hannah Riley Knight** — Pritzker School of Molecular Engineering, University of Chicago, Chicago, Illinois 60637, United States

**Nakisha S. Rutledge** — Pritzker School of Molecular Engineering, University of Chicago, Chicago, Illinois 60637, United States

**Bradley Studnitzer** — Pritzker School of Molecular Engineering, University of Chicago, Chicago, Illinois 60637, United States;

Department of Chemistry, University of Chicago, Chicago, Illinois 60637, United States

**Stuart J. Rowan** — Pritzker School of Molecular Engineering, University of Chicago, Chicago, Illinois 60637, United States; Department of Chemistry, University of Chicago, Chicago, Illinois 60637, United States;  [orcid.org/0000-0001-8176-0594](https://orcid.org/0000-0001-8176-0594)

Complete contact information is available at: <https://pubs.acs.org/10.1021/acs.jmedchem.4c00516>

### Author Contributions

A.M.W. and M.A.L. contributed equally. A.M.W. and A.P.E.-K. conceived the study. Preliminary high throughput screening was conducted by M.G.R., J.Y.K., J.S., and Q.C. *In vitro* assays were conducted by A.M.W., M.A.L., Q.C., and N.S.R. Synthesis and formulation studies were conducted by A.M.W., J.Y.K., and T.U. Vaccination studies were conducted by A.M.W., M.A.L., M.G.R., J.S., T.U., U.M.I., H.R.K., N.S.R., and B.S. Tumor studies were conducted by M.A.L., Q.C., and J.S. The work was supervised by S.J.R. and A.P.E.-K. The manuscript was prepared by A.M.W., M.A.L., S.J.R., and A.P.E.-K. with input from all authors.

### Notes

The authors declare no competing financial interest.

## ■ ACKNOWLEDGMENTS

All of us acknowledge support from an NIH adjuvant discovery contract (75N93019C00041), an NIH adjuvant development contract (75N93023C00044), and DTRA (1-18-1-0052). A.M.W. acknowledges partial support from NIH T32 GM008720. We thank University of Chicago veterinary technicians for exceptional animal care and Sam Marsden for assistance with variable temperature NMR. The authors also thank the UChicago Cytometry and Antibody Technology Facility (NIH P30CA014599), Materials Research Science and Engineering Center (NSF DMR 2011854), Cellular Screening Center (RRID:SCR\_017914), NMR Core Facility, and Advanced Electron Microscopy Facility for instrumentation and support. The Table of Contents figure was created using BioRender.com.

## ■ ABBREVIATIONS USED

NLRP3, NLR family pyrin domain containing 3; TLR, Toll-like receptor; GSDMD, gasdermin D; Casp1, caspase-1; PRR, pattern recognition receptor; LPS, lipopolysaccharide; BMDM, bone marrow derived macrophage; LDH, lactate dehydrogenase; ELISA, enzyme-linked immunosorbent assay; BMDC, bone marrow derived dendritic cell; CDK, cyclin-dependent kinase; SASP, senescence associated secretory phenotype; DPI, diphenyliodonium chloride; NSA, necrosulfonamide; MLKL, mixed lineage kinase domain like; Nec-1, necrostatin 1; IL-1R, IL-1 receptor; KO, knockout; NF- $\kappa$ B, nuclear factor kappa-light-chain-enhancer of activated B cells; OVA, ovalbumin; MPLA, monophosphoryl lipid A; API, active pharmaceutical ingredient; DPPE, 1,2-dipalmitoyl-*sn*-glycero-3-phosphoethanolamine; Ribo-L, ribociclib, lipid modified; Ribo-F, ribociclib, free; DSpC, 1,2-distearoyl-*sn*-glycero-3-phosphatidylcholine; MHC-II, major histocompatibility complex II; ER, estrogen receptor; HER2, human epidermal growth factor receptor 2; PBS, phosphate buffered saline; TBS-T, tris buffered saline with Tween-20; SDS-PAGE, sodium dodecyl sulfate polyacrylamide gel chromatography; PVDF, poly(vinylidene difluoride); RT, room temperature; HRP, horseradish peroxidase; BSA, bovine

serum albumin; PEG300, poly(ethylene glycol); average Mn, 300 g/mol; DMSO, dimethyl sulfoxide

## ■ REFERENCES

(1) Pulendran, B.; Arunachalam, P. S.; O'Hagan, D. T. Emerging concepts in the science of vaccine adjuvants. *Nat. Rev. Drug Discov.* **2021**, *20* (6), 454–475.

(2) Marty-Roix, R.; Vladimer, G. I.; Pouliot, K.; Weng, D.; Buglione-Corbett, R.; West, K.; MacMicking, J. D.; Chee, J. D.; Wang, S.; Lu, S.; Lien, E. Identification of QS-21 as an Inflammasome-activating Molecular Component of Saponin Adjuvants. *J. Biol. Chem.* **2016**, *291* (3), 1123–36.

(3) Welsby, I.; Detienne, S.; N'Kuli, F.; Thomas, S.; Wouters, S.; Bechtold, V.; De Wit, D.; Gineste, R.; Reinheckel, T.; Elouahabi, A.; Courtoy, P. J.; Didierlaurent, A. M.; Goriely, S. Lysosome-Dependent Activation of Human Dendritic Cells by the Vaccine Adjuvant QS-21. *Front Immunol* **2017**, *7*, 663.

(4) Coccia, M.; Collignon, C.; Herve, C.; Chalon, A.; Welsby, I.; Detienne, S.; van Helden, M. J.; Dutta, S.; Genito, C. J.; Waters, N. C.; Van Deun, K.; Smilde, A. K.; van den Berg, R. A.; Franco, D.; Bourguignon, P.; Morel, S.; Garcon, N.; Lambrecht, B. N.; Goriely, S.; van der Most, R.; Didierlaurent, A. M. Cellular and molecular synergy in AS01-adjutanted vaccines results in an early IFNgamma response promoting vaccine immunogenicity. *NPJ. Vaccines* **2017**, *2*, 25.

(5) Deets, K. A.; Vance, R. E. Inflammasomes and adaptive immune responses. *Nat. Immunol* **2021**, *22*, 412–422.

(6) Sharma, B. R.; Kanneganti, T. D. NLRP3 inflammasome in cancer and metabolic diseases. *Nat. Immunol* **2021**, *22* (5), 550–559.

(7) Rodrigues, T. S.; de Sa, K. S. G.; Ishimoto, A. Y.; Becerra, A.; Oliveira, S.; Almeida, L.; Goncalves, A. V.; Perucello, D. B.; Andrade, W. A.; Castro, R.; Veras, F. P.; Toller-Kawahisa, J. E.; Nascimento, D. C.; de Lima, M. H. F.; Silva, C. M. S.; Caetite, D. B.; Martins, R. B.; Castro, I. A.; Pontelli, M. C.; de Barros, F. C.; do Amaral, N. B.; Giannini, M. C.; Bonjorno, L. P.; Lopes, M. I. F.; Santana, R. C.; Vilar, F. C.; Auxiliadora-Martins, M.; Luppino-Assad, R.; de Almeida, S. C. L.; de Oliveira, F. R.; Batah, S. S.; Siyuan, L.; Benatti, M. N.; Cunha, T. M.; Alves-Filho, J. C.; Cunha, F. Q.; Cunha, L. D.; Frantz, F. G.; Kohlsdorf, T.; Fabro, A. T.; Arruda, E.; de Oliveira, R. D. R.; Louzada-Junior, P.; Zamboni, D. S. Inflammasomes are activated in response to SARS-CoV-2 infection and are associated with COVID-19 severity in patients. *J. Exp Med.* **2021**, *218*, No. e20201707.

(8) Ising, C.; Venegas, C.; Zhang, S.; Scheiblich, H.; Schmidt, S. V.; Vieira-Saecker, A.; Schwartz, S.; Albasset, S.; McManus, R. M.; Tejera, D.; Griep, A.; Santarelli, F.; Brosseron, F.; Opitz, S.; Stüden, J.; Merten, M.; Kayed, R.; Golenbock, D. T.; Blum, D.; Latz, E.; Buee, L.; Heneka, M. T. NLRP3 inflammasome activation drives tau pathology. *Nature* **2019**, *575* (7784), 669–673.

(9) Martinon, F.; Petrilli, V.; Mayor, A.; Tardivel, A.; Tschopp, J. Gout-associated uric acid crystals activate the NALP3 inflammasome. *Nature* **2006**, *440* (7081), 237–41.

(10) Hatscher, L.; Lehmann, C. H. K.; Purbojo, A.; Onderka, C.; Liang, C.; Hartmann, A.; Cesnjevar, R.; Bruns, H.; Gross, O.; Nimmerjahn, F.; Ivanovic-Burmazovic, I.; Kunz, M.; Heger, L.; Dudziak, D. Select hyperactivating NLRP3 ligands enhance the TH1- and TH17-inducing potential of human type 2 conventional dendritic cells. *Sci. Signal* **2021**, *14*, 680.

(11) Papi, A.; Ison, M. G.; Langley, J. M.; Lee, D. G.; Leroux-Roels, I.; Martinon-Torres, F.; Schwarz, T. F.; van Zyl-Smit, R. N.; Campora, L.; Dezutter, N.; de Schrevel, N.; Fissette, L.; David, M. P.; Van der Wielen, M.; Kostanyan, L.; Hulstrom, V. Respiratory Syncytial Virus Prefusion F Protein Vaccine in Older Adults. *N Engl J. Med.* **2023**, *388*, 595–608.

(12) Lal, H.; Cunningham, A. L.; Godeaux, O.; Chlibek, R.; Diez-Domingo, J.; Hwang, S. J.; Levin, M. J.; McElhaney, J. E.; Poder, A.; Puig-Barbera, J.; Vesikari, T.; Watanabe, D.; Weckx, L.; Zahaf, T.; Heineman, T. C. Efficacy of an adjuvanted herpes zoster subunit vaccine in older adults. *N Engl J. Med.* **2015**, *372*, 2087.

(13) RTS, S. C. T. P.. Efficacy and safety of RTS,S/AS01 malaria vaccine with or without a booster dose in infants and children in Africa: final results of a phase 3, individually randomised, controlled trial. *Lancet* **2015**, *386* (9988), 31–45.

(14) Heath, P. T.; Galiza, E. P.; Baxter, D. N.; Boffito, M.; Browne, D.; Burns, F.; Chadwick, D. R.; Clark, R.; Cosgrove, C.; Galloway, J.; Goodman, A. L.; Heer, A.; Higham, A.; Iyengar, S.; Jamal, A.; Jeanes, C.; Kalra, P. A.; Kyriakidou, C.; McAuley, D. F.; Meyrick, A.; Minassian, A. M.; Minton, J.; Moore, P.; Munsoor, I.; Nicholls, H.; Osanlou, O.; Packham, J.; Pretswell, C. H.; San Francisco Ramos, A.; Saralaya, D.; Sheridan, R. P.; Smith, R.; Soiza, R. L.; Swift, P. A.; Thomson, E. C.; Turner, J.; Viljoen, M. E.; Albert, G.; Cho, I.; Dubovsky, F.; Glenn, G.; Rivers, J.; Robertson, A.; Smith, K.; Toback, S. Safety and Efficacy of NVX-CoV2373 Covid-19 Vaccine. *N Engl J. Med.* **2021**, *385*, 1172–1183.

(15) Wang, P.; Kim, Y. J.; Navarro-Villalobos, M.; Rohde, B. D.; Gin, D. Y. Synthesis of the potent immunostimulatory adjuvant QS-21A. *J. Am. Chem. Soc.* **2005**, *127* (10), 3256–7.

(16) Fernandez-Tejada, A.; Tan, D. S.; Gin, D. Y. Development of Improved Vaccine Adjuvants Based on the Saponin Natural Product QS-21 through Chemical Synthesis. *Acc. Chem. Res.* **2016**, *49* (9), 1741–56.

(17) Guan, Y.; Omueti-Ayoade, K.; Mutha, S. K.; Hergenrother, P. J.; Tapping, R. I. Identification of novel synthetic toll-like receptor 2 agonists by high throughput screening. *J. Biol. Chem.* **2010**, *285* (31), 23755–62.

(18) Chan, M.; Hayashi, T.; Mathewson, R. D.; Nour, A.; Hayashi, Y.; Yao, S.; Tawatao, R. I.; Crain, B.; Tsigelny, I. F.; Kouznetsova, V. L.; Messer, K.; Pu, M.; Corr, M.; Carson, D. A.; Cottam, H. B. Identification of substituted pyrimido[5,4-b]indoles as selective Toll-like receptor 4 ligands. *J. Med. Chem.* **2013**, *56* (11), 4206–23.

(19) Liu, B.; Tang, L.; Zhang, X.; Ma, J.; Sehgal, M.; Cheng, J.; Zhang, X.; Zhou, Y.; Du, Y.; Kulp, J.; Guo, J. T.; Chang, J. A cell-based high throughput screening assay for the discovery of cGAS-STING pathway agonists. *Antiviral Res.* **2017**, *147*, 37–46.

(20) Kim, J. Y.; Rosenberger, M. G.; Chen, S.; Ip, C. K.; Bahmani, A.; Chen, Q.; Shen, J.; Tang, Y.; Wang, A.; Kenna, E.; Son, M.; Tay, S.; Ferguson, A. L.; Esser-Kahn, A. P. Discovery of New States of Immunomodulation for Vaccine Adjuvants via High Throughput Screening: Expanding Innate Responses to PRRs. *ACS Cent Sci.* **2023**, *9* (3), 427–439.

(21) Henriksen, B. D.; Tamrakar, A. K.; Phulka, J. S.; Barra, N. G.; Schertzer, J. D. Statins activate the NLRP3 inflammasome and impair insulin signaling via p38 and mTOR. *Am. J. Physiol Endocrinol Metab* **2020**, *319* (1), E110–E116.

(22) Henriksen, B. D.; Lau, T. C.; Cavallari, J. F.; Denou, E.; Chi, W.; Lally, J. S.; Crane, J. D.; Duggan, B. M.; Foley, K. P.; Fullerton, M. D.; Tarnopolsky, M. A.; Steinberg, G. R.; Schertzer, J. D. Fluvastatin causes NLRP3 inflammasome-mediated adipose insulin resistance. *Diabetes* **2014**, *63* (11), 3742–7.

(23) Satoh, M.; Tabuchi, T.; Itoh, T.; Nakamura, M. NLRP3 inflammasome activation in coronary artery disease: results from prospective and randomized study of treatment with atorvastatin or rosuvastatin. *Clinical Science* **2014**, *126* (3), 233–241.

(24) Hajek, E.; Krebs, F.; Bent, R.; Haas, K.; Bast, A.; Steinmetz, I.; Tuettenberg, A.; Grabbe, S.; Bros, M. BRAF inhibitors stimulate inflammasome activation and interleukin 1 beta production in dendritic cells. *Oncotarget* **2018**, *9* (47), 28294–28308.

(25) Malumbres, M.; Barbacid, M. Cell cycle, CDKs and cancer: a changing paradigm. *Nat. Rev. Cancer* **2009**, *9* (3), 153–66.

(26) Klein, M. E.; Kovatcheva, M.; Davis, L. E.; Tap, W. D.; Koff, A. CDK4/6 Inhibitors: The Mechanism of Action May Not Be as Simple as Once Thought. *Cancer Cell* **2018**, *34* (1), 9–20.

(27) Fassl, A.; Geng, Y.; Sicinski, P. CDK4 and CDK6 kinases: From basic science to cancer therapy. *Science* **2022**, *375*, No. eabc1495.

(28) Acosta, J. C.; Banito, A.; Wuestefeld, T.; Georgilis, A.; Janich, P.; Morton, J. P.; Athineos, D.; Kang, T. W.; Lasitschka, F.; Andrusis, M.; Pascual, G.; Morris, K. J.; Khan, S.; Jin, H.; Dharmalingam, G.; Snijders, A. P.; Carroll, T.; Capper, D.; Pritchard, C.; Inman, G. J.; Longerich, T.; Sansom, O. J.; Benitah, S. A.; Zender, L.; Gil, J. A complex secretory

program orchestrated by the inflammasome controls paracrine senescence. *Nat. Cell Biol.* **2013**, *15* (8), 978–90.

(29) Faget, D. V.; Ren, Q.; Stewart, S. A. Unmasking senescence: context-dependent effects of SASP in cancer. *Nat. Rev. Cancer* **2019**, *19* (8), 439–453.

(30) Goel, S.; DeCristo, M. J.; Watt, A. C.; BrinJones, H.; Sceneay, J.; Li, B. B.; Khan, N.; Ubellacker, J. M.; Xie, S.; Metzger-Filho, O.; Hoog, J.; Ellis, M. J.; Ma, C. X.; Ramm, S.; Krop, I. E.; Winer, E. P.; Roberts, T. M.; Kim, H. J.; McAllister, S. S.; Zhao, J. J. CDK4/6 inhibition triggers anti-tumour immunity. *Nature* **2017**, *548* (7668), 471–475.

(31) Deng, J.; Wang, E. S.; Jenkins, R. W.; Li, S.; Dries, R.; Yates, K.; Chhabra, S.; Huang, W.; Liu, H.; Aref, A. R.; Ivanova, E.; Paweletz, C. P.; Bowden, M.; Zhou, C. W.; Herter-Sprie, G. S.; Sorrentino, J. A.; Bisi, J. E.; Lizotte, P. H.; Merlin, A. A.; Quinn, M. M.; Bufe, L. E.; Yang, A.; Zhang, Y.; Zhang, H.; Gao, P.; Chen, T.; Cavanaugh, M. E.; Rode, A. J.; Haines, E.; Roberts, P. J.; Strum, J. C.; Richards, W. G.; Lorch, J. H.; Parangi, S.; Gunda, V.; Boland, G. M.; Bueno, R.; Palakurthi, S.; Freeman, G. J.; Ritz, J.; Haining, W. N.; Sharpless, N. E.; Arthanari, H.; Shapiro, G. I.; Barbie, D. A.; Gray, N. S.; Wong, K. K. CDK4/6 Inhibition Augments Antitumor Immunity by Enhancing T-cell Activation. *Cancer Discov* **2018**, *8* (2), 216–233.

(32) Petroni, G.; Formenti, S. C.; Chen-Kiang, S.; Galluzzi, L. Immunomodulation by anticancer cell cycle inhibitors. *Nat. Rev. Immunol.* **2020**, *20* (11), 669–679.

(33) Heckler, M.; Ali, L. R.; Clancy-Thompson, E.; Qiang, L.; Ventre, K. S.; Lenehan, P.; Roehle, K.; Luoma, A.; Boelaars, K.; Peters, V.; McCreary, J.; Boschert, T.; Wang, E. S.; Suo, S.; Marangoni, F.; Mempel, T. R.; Long, H. W.; Wucherpfennig, K. W.; Dougan, M.; Gray, N. S.; Yuan, G. C.; Goel, S.; Tolaney, S. M.; Dougan, S. K. Inhibition of CDK4/6 Promotes CD8 T-cell Memory Formation. *Cancer Discov* **2021**, *11* (10), 2564–2581.

(34) Jin, X.; Ding, D.; Yan, Y.; Li, H.; Wang, B.; Ma, L.; Ye, Z.; Ma, T.; Wu, Q.; Rodrigues, D. N.; Kohli, M.; Jimenez, R.; Wang, L.; Goodrich, D. W.; de Bono, J.; Dong, H.; Wu, H.; Zhu, R.; Huang, H. Phosphorylated RB Promotes Cancer Immunity by Inhibiting NF- $\kappa$ B Activation and PD-L1 Expression. *Mol. Cell* **2019**, *73* (1), 22.

(35) Kumar, A.; Ramani, V.; Bharti, V.; de Lima Bellan, D.; Saleh, N.; Uzhachenko, R.; Shen, C.; Arteaga, C.; Richmond, A.; Reddy, S. M.; Vilgelm, A. Dendritic cell therapy augments antitumor immunity triggered by CDK4/6 inhibition and immune checkpoint blockade by unleashing systemic CD4 T-cell responses. *J. Immunother. Cancer* **2023**, *11*, e006019.

(36) McKee, C. M.; Coll, R. C. NLRP3 inflammasome priming: A riddle wrapped in a mystery inside an enigma. *J. Leukoc. Biol.* **2020**, *108* (3), 937–952.

(37) Swanson, K. V.; Deng, M.; Ting, J. P. The NLRP3 inflammasome: molecular activation and regulation to therapeutics. *Nat. Rev. Immunol.* **2019**, *19* (8), 477–489.

(38) Grootjans, S.; Vanden Berghe, T.; Vandenabeele, P. Initiation and execution mechanisms of necroptosis: an overview. *Cell Death Differ.* **2017**, *24* (7), 1184–1195.

(39) Herranz, N.; Gil, J. Mechanisms and functions of cellular senescence. *J. Clin. Invest.* **2018**, *128* (4), 1238–1246.

(40) Johnson, A. G.; Tomai, M.; Solem, L.; Beck, L.; Ribi, E. Characterization of a nontoxic monophosphoryl lipid A. *Rev. Infect. Dis.* **1987**, *9*, S512.

(41) Weiss, A. M.; Hossainy, S.; Rowan, S. J.; Hubbell, J. A.; Esser-Kahn, A. P. Immunostimulatory Polymers as Adjuvants, Immunotherapies, and Delivery Systems. *Macromolecules* **2022**, *55* (16), 6913–6937.

(42) Kraft, J. C.; Freeling, J. P.; Wang, Z.; Ho, R. J. Emerging research and clinical development trends of liposome and lipid nanoparticle drug delivery systems. *J. Pharm. Sci.* **2014**, *103* (1), 29–52.

(43) Tao, X.; Jia, N.; Cheng, N.; Ren, Y.; Cao, X.; Liu, M.; Wei, D.; Wang, F. Q. Design and evaluation of a phospholipase D based drug delivery strategy of novel phosphatidyl-prodrug. *Biomaterials* **2017**, *131*, 1–14.

(44) Rondla, R.; PadmaRao, L. S.; Ramatenki, V.; Haredi-Abdel-Monsef, A.; Potlapally, S. R.; Vuruputuri, U. Selective ATP competitive leads of CDK4: Discovery by 3D-QSAR pharmacophore mapping and molecular docking approach. *Comput. Biol. Chem.* **2017**, *71*, 224–229.

(45) Li, A. W.; Sobral, M. C.; Badrinath, S.; Choi, Y.; Graveline, A.; Stafford, A. G.; Weaver, J. C.; Dellacherie, M. O.; Shih, T. Y.; Ali, O. A.; Kim, J.; Wucherpfennig, K. W.; Mooney, D. J. A facile approach to enhance antigen response for personalized cancer vaccination. *Nat. Mater.* **2018**, *17* (6), 528–534.

(46) Tripathy, D.; Im, S. A.; Colleoni, M.; Franke, F.; Bardia, A.; Harbeck, N.; Hurvitz, S. A.; Chow, L.; Sohn, J.; Lee, K. S.; Campos-Gomez, S.; Villanueva Vazquez, R.; Jung, K. H.; Babu, K. G.; Wheatley-Price, P.; De Laurentiis, M.; Im, Y. H.; Kuemmel, S.; El-Saghier, N.; Liu, M. C.; Carlson, G.; Hughes, G.; Diaz-Padilla, I.; Germa, C.; Hirawat, S.; Lu, Y. S. Ribociclib plus endocrine therapy for premenopausal women with hormone-receptor-positive, advanced breast cancer (MONALEE-SA-7): a randomised phase 3 trial. *Lancet Oncol.* **2018**, *19* (7), 904–915.

(47) Saxena, M.; van der Burg, S. H.; Melief, C. J. M.; Bhardwaj, N. Therapeutic cancer vaccines. *Nat. Rev. Cancer* **2021**, *21* (6), 360–378.

(48) Kozar, K.; Cierny, M. A.; Rebel, V. I.; Shigematsu, H.; Zagordzon, A.; Sicinska, E.; Geng, Y.; Yu, Q.; Bhattacharya, S.; Bronson, R. T.; Akashi, K.; Sicinski, P. Mouse development and cell proliferation in the absence of D-cyclins. *Cell* **2004**, *118* (4), 477–491.

(49) Malumbres, M.; Sotillo, R.; Santamaría, D.; Galan, J.; Cerezo, A.; Ortega, S.; Dubus, P.; Barbacid, M. Mammalian cells cycle without the D-type cyclin-dependent kinases Cdk4 and Cdk6. *Cell* **2004**, *118* (4), 493–504.

(50) Tahtinen, S.; Tong, A. J.; Himmels, P.; Oh, J.; Paler-Martinez, A.; Kim, L.; Wicha, S.; Oei, Y.; McCarron, M. J.; Freund, E. C.; Amir, Z. A.; de la Cruz, C. C.; Haley, B.; Blanchette, C.; Schartner, J. M.; Ye, W.; Yadav, M.; Sahin, U.; Delamarre, L.; Mellman, I. IL-1 and IL-1ra are key regulators of the inflammatory response to RNA vaccines. *Nat. Immunol.* **2022**, *23* (4), 532–542.

(51) Poratti, M.; Marzaro, G. Third-generation CDK inhibitors: A review on the synthesis and binding modes of Palbociclib, Ribociclib and Abemaciclib. *Eur. J. Med. Chem.* **2019**, *172*, 143–153.

(52) Manna, S.; Howitz, W. J.; Oldenhuis, N. J.; Eldredge, A. C.; Shen, J.; Nihesh, F. N.; Lodoen, M. B.; Guan, Z.; Esser-Kahn, A. P. Immunomodulation of the NLRP3 Inflammasome through Structure-Based Activator Design and Functional Regulation via Lysosomal Rupture. *ACS Cent. Sci.* **2018**, *4* (8), 982–995.

(53) Ajit, J.; Cassaidy, B.; Tang, S.; Solanki, A.; Chen, Q.; Shen, J.; Esser Kahn, A. P. Temporal Control of Trained Immunity via Encapsulated Release of beta-Glucan Improves Therapeutic Applications. *Adv. Healthc Mater.* **2022**, *11*, No. e2200819.

(54) Garçon, N.; Chomez, P.; Van Mechelen, M. GlaxoSmithKline Adjuvant Systems in vaccines: concepts, achievements and perspectives. *Expert Rev. Vaccines* **2007**, *6* (5), 723–39.